LANGMUIR

Article

Linear chain formation of split-aptamer dimers on surfaces triggered by adenosine

Chenze Lu, Christine Saint-Pierre, Didier Gasparutto, Yoann Roupioz, Eric Peyrin, and Arnaud Buhot

Langmuir, **Just Accepted Manuscript** • DOI: 10.1021/acs.langmuir.7b02104 • Publication Date (Web): 16 Oct 2017

ACS Publications

Langmuir is published by the American Chemical Society. 1155 Sixteenth Street N.W., Washington, DC 20036

Linear chain formation of split-aptamer dimers on surfaces triggered by adenosine

Chenze Lu[1,2], Christine Saint-Pierre[1], Didier Gasparutto[1], Yoann Roupioz[1], Eric Peyrin[2] and Arnaud Buhot[1].

1 Univ. Grenoble Alpes, CEA, CNRS, INAC, SyMMES, F-38000 Grenoble, France

2 Univ. Grenoble Alpes, CNRS, DPM, F-38000 Grenoble, France

KEYWORDS. Aptamer, small ligand, adenosine, linear chains, grafting density.

ABSTRACT. The detection of small molecules impacts various fields however their small size and low concentration are usually the cause of limitations in their detection. Thus, the need for biosensors with appropriate probes and signal amplification strategies is required. Aptamers are appropriate probes selected specifically against small targets like adenosine. The possibility to split aptamers in parts led to original amplification strategies based on sandwich assays. By combining the self-assembling of oligonucleotide dimers with split-aptamer dangling ends and Surface Plasmon Resonance imaging technique, we developed an original amplification approach based on linear chain formation in presence of the adenosine target. In this paper, based on sequence engineering, we analyzed its performance and the effect of probe grafting density on the length of the chains formed at the surface of the biosensor.

Introduction

The detection of small molecules plays an important role in various fields such as food safety, disease diagnosis, homeland security and environmental control (1, 2, 3). While the detection of proteins or macromolecules is accessible through direct recognition by antibodies or by sandwich assays like in ELISA, the small size of analytes and their low concentration in matrices usually constitute an impediment for their sensing. Current research focus on the development and use of alternative probes such as aptamers to overcome the difficulties to raise antibodies against small molecules (4). Aptamers are single stranded oligonucleotide chains selected specifically against their target by the SELEX method (5, 6). The folding of the aptamers give rise to the specificity and selectivity towards the target ligand. Besides the use of adequate probes, the development of label-free biosensors against small targets usually requires indirect signal amplification due to the small signal obtained from the direct binding of the small targets to the probes. In this respect, Surface Plasmon Resonance imaging (SPRi) is an optical transduction technique sensitive to the change of refractive index at proximity of a gold surface. It provides a real-time monitoring of the surface environment allowing the follow-up of bio-molecular interactions without requiring any labeling of the targets. The direct detection of small molecules (molecular weight less than 1 kDa) by SPRi is however challenging since the signal is proportional to the change of mass brought by the targets binding to the probes grafted on the gold surface. Indirect strategies are commonly used to achieve efficient detection either by using plasmonic effects and sandwich assays with gold nanoparticles or by self-assembling strategies like the use of Hybridization Chain Reactions (HCR) (7, 8, 9, 10, 11, 12, 13, 14, 15, 16, 17).

Adenosine is a component of many biological cofactors. It plays an important part in many biochemical processes, for example, the energy transfer between Adenosine triphosphate (ATP)

and Adenosine diphosphate (ADP) or in the signal transduction as cyclic Adenosine monophosphate (cAMP) (18). It is also involved in promoting sleep and regulation of blood flow. (19, 20) The detection of Adenosine could be helpful for medical research concerning these interactions. Moreover, Adenosine is a small molecule model for which an aptamer has been previously selected by Huizenga and Szostak (21). Due to the hairpin structure of the aptamer and the presence of the binding pocket within the stem, the aptamer may be split within the loop into two different strands without strongly affecting the binding affinity towards the adenosine ligand. The two split-aptamers may thus be used under a sandwich-like format similarly as two antibodies in Enzyme Linked Immuno-Sorbent Assay (ELISA) detection (22, 23, 24, 25, 26, 27, 28). Solution phase detection have been developed using split-aptamers grafted to Gold nanoparticles for colorimetric detection (23). On solid support, electrochemical detection have been developed where one strand of the split-aptamer couple was grafted to the surface and the other strand incorporated a redox label (24, 25). In previous work, we introduced functionalized gold nanoparticles into the detection process. These gold nanoparticles increased the signal in two ways, the mass effect and the coupling effect between the localized surface plasmon of the particles and the surface plasmon of the gold prism (26, 28). To avoid the complex synthesis and functionalization of gold nanoparticles, we developed herein an original approach based on the self-assembling of oligonucleotide dimers with split-aptamer dangling ends forming linear chains in presence of the adenosine target. In our assay inspired from the HCR approach, the linear chain formation was triggered by the small molecules thanks to split-aptamer sandwiches instead of the commonly used DNA hybridization in HCR. This formation of linear chains on the biosensor surface served as an amplification strategy. In this paper, we evaluated its performance in term of

detection as well as the effect of the probe grafting density on the length of the linear chains formed at the surface of the biosensor.

Materials and methods

Oligonucleotides and reagent solutions

Adenosine and guanosine as well as all the reagents used to prepare the buffer were purchased from Sigma-Aldrich (Saint Quentin Fallavier, France). CH_3O-PEG-SH (PEG 2000, MW 2000 Da) was purchased from Rapp Polymere GmbH (Tübingen, Germany). Two different buffers were used in this work: the SPR running buffer (HEPES 10 mM, $MgCl_2$ 5 mM, NaCl 150 mM, pH 7.4) and the grafting buffer (K_2HPO_4 1 M, pH 9.25). Furthermore, we used a solution of NaOH at 50 mM for a complete regeneration of the microarray. The water used was ultrapure with 18.2 MΩ·cm resistivity.

The oligonucleotides were purchased from Eurogentec (Angers, France). Those used for the functionalization of the gold surface had a thiol modification at the 5' end position. Details of the sequences are displayed in Table 1. In the names of the sequences, "S" is an abbreviation for split-aptamer and "Z" for zipper. "SX" and "SX*" are two half sequences of the adenosine aptamer that have been split while keeping their binding properties (26, 28). The symbol "X" relates to the number of hybridizing bases of the stem part with X = 5, 6 and 8 (blue sequences in Table 1). The binding pocket of the split-aptamers (bold black in Table 1) have not been affected during the sequence engineering to avoid loss of affinity towards adenosine. For the sequences S5Z and S5*Zc, an additional GAG sequence was present flanking the split aptamers. Those non hybridizing ends were preventing from the possibility to link monomers by enzymatic reactions. Those sequences were removed for the other monomer sequences. S6c correspond to the

complementary sequence of S6. Similarly, "Z" and "Zc" are two complementary sequences in order to form hybridizing dimers in solution (see Fig.1A). For example, "S5Z" is the combination of the two sequences S5 and Z. S5*Zc is the combination of the other split half S5* of the adenosine aptamer with 5 hybridizing pairs on the stem. While S5Z and S5*Zc are mixed in solution, Zc hybridizes to its complementary sequence Z to form the S5 dimer. Similarly S6 dimers are formed by mixtures of S6Z and S6*Zc. When S6Z and S6cZc are mixed, linear chains may be formed in solution due to both hybridization of the complementary sequences Z/Zc and S6/S6c.

Name	Sequence 5' to 3'
S5Z	TGC**GGAGGA**AGGTTGAG*GACCATCGTGCGGGTAGGTAGACC*
S5*Zc	GAGAACCT**GGGGGAG**TA*GGTCTACCTACCCGCACGATGGTC*
S6Z	CCTGC**GGAGGA**AGGTTC*GACCATCGTGCGGGTAGGTAGA*
S6*Zc	GAACCT**GGGGGAG**TAGG*TCTACCTACCCGCACGATGGTC*
S8Z	CCTGC**GGAGGA**AGGTTCTC*GACCATCGTGCGGGTAGGTAGA*
S8*Zc	GAGAACCT**GGGGGAG**TAGG*TCTACCTACCCGCACGATGGTC*
S6cZc	GAACCTTCCTCCGCAGG*TCTACCTACCCGCACGATGGTC*
Z	HS-*GACCATCGTGCGGGTAGGTAGA*CC
NC	HS-TGCGATCGCAGCGGTAACCTGACC

Table 1: Oligonucleotide sequences used in this work. S stands for split-aptamer sequences and Z for zipper sequences. Blue bold: Hybridization part of the split aptamers. Red italic: Zipper sequences for dimer hybridization. Black bold: Binding pocket of adenosine. NC Negative control sequence.

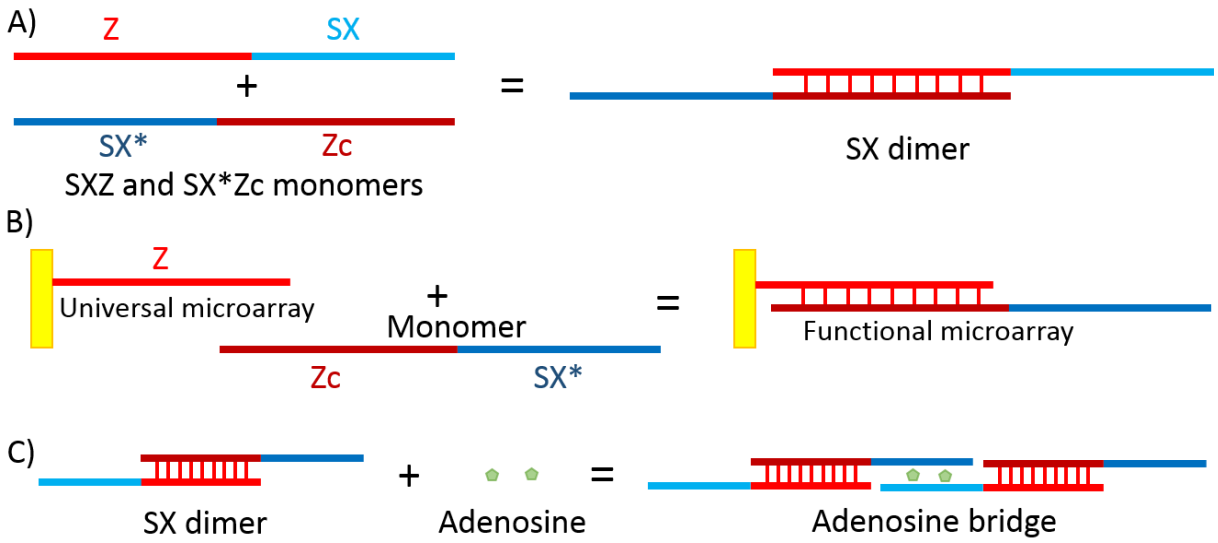

Figure 1 Scheme of the strands and their interactions. A) Monomer strands formed of Z+SX and Zc+SX* with X = 5, 6 or 8 complementary bases between SX and SX*. SX* may also be replaced by SXc the fully complementary strand of SX. Due to the fully complementary strands Z and Zc, the two monomers form dimers in solution. B) From an initial microarray with Z strand probes at various grafting densities, a functional microarray may be obtained by the injection of monomers SX*Zc leading to SX* dangling end probes. C) The addition of adenosine target in presence of dimers on functional microarrays allows for the formation of linear chains by adenosine bridges.

Biosensor functionalization with varying grafting densities

Self-Assembled Monolayers (SAM) of oligonucleotides with thiol moiety at the 5' end were formed on gold-coated prisms (Horiba Scientific-GenOptics, Orsay, France) following previously described protocols (26, 28, 29, 30). In brief, the gold surface on top of the prism was cleaned with plasma treatment (0.6 mbar, 75% Oxygen, 25% Argon, power 40 W, 3 min) using a Femto plasma generator (Diener Electronic, Ebhausen, Germany). The grafting solution was spotted onto the surface with a piezoelectric dispensing system sciFLEXARRAYER S3 (Scienion, Berlin,

Germany) which provided precise control of position and volume (4 nL) of the droplets (see Supplementary Information (SI) Fig. S1). The grafting solution consisted of K_2HPO_4 buffer (1 M, pH 9.25) with PEG2000 (10 μM) and a mixture of thiolated DNA strands. The atmosphere in which the deposition took place had a controlled humidity of 85%. The prism was left in the same humid chamber for 2 hours after the deposition. Later the prism was removed from the chamber and kept overnight in dark and dry environment to complete the formation of the SAMs. The second morning, the prism was taken out, the gold surface was rinsed with deionized water and dried with argon flow. The diameters of the spots were around 500 μm and the total grafting density is 8 pmol/cm^{-2}. The density of the grafted probes (Z) was controlled by diluting the strands Z with negative control NC strands while keeping the total strand concentration at 20 μM. Thus, the probes density varied from 0.4, 0.8, 2, 4 to 8 pmol/cm^{-2} corresponding to the following ratio of Z probes with respect to the total DNA strands (1/20, 1/10, 1/4, 1/2 and 1). For reproducibility studies, at least triplicate spots of each grafting density of probes have been deposited and several microarrays have been produced and analyzed. Before the first use, the functionalized gold surface was immersed in 150 μM of PEG2000 solution for 90 min at room temperature to block the surface from non-specific interactions. After this blocking procedure, the surface was rinsed again with deionized water and dried with argon flow. Between successive experiments, the microarrays were stored dry at 4 °C. From those initial microarrays with Z probes, the injection of SX*Zc strands lead to a functional microarrays upon hybridization of the Z and Zc strands leading SX* strands as dangling end probes (see Fig.1B). Thus, the same microarray served to analyze the sequence engineering of split-aptamers with 5, 6 or 8 hybridizing complementary bases (probes S5*, S6* or S8* respectively).

SPRi measurement

The SPRi apparatus used for the experiments was the SPRi-Lab from Horiba Scientific-GenOptics with incoherent light source (λ = 635 nm) as in our previous works (26, 28). The flowing solution was first pumped (syringe Cavro pump, Tecan, San Jose, CA, USA) into a degassing system from Alltech (Carquefou, France) and then continued into the reaction chamber which consisted in a hexagonal reactor PEEK flow cell with approximately 15 µL of volume. The temperature was set at 25 °C for all the experiments. Before each injection, the solution to be injected was loaded into a 1 mL injection loop. The SPR data were acquired using the software from Horiba Scientific-GenOptics. Before any injection, the grafted spots are detected on the image of the camera. Then, a portion of each surface of the spots is selected for averaging the reflectivity signal. Finally, during the various injections, the images of the microarray and the averaged reflectivity signals for each spots are acquired in real time (see an example of SPR image following an injection in SI Fig. S2). In the following, the changes in reflectivity ΔR (in %) were obtained by the average over the triplicate spot measurements on the same microarray.

The buffer used during the SPRi measurement contained 10 mM HEPES, 5 mM $MgCl_2$ and 150 mM NaCl, the pH of the solution was adjusted to 7.4. The DNA strands to be injected were first mixed in the tube and the buffer was added along with adenosine solution. The mixture was then heated to 90 °C for 5 min and cooled down for 30 min before use. The concentration of the DNA strands was fixed at 1 µM in all the experiments whereas the concentration of adenosine varied depending on the purpose. Injection of Guanosine at 1 mM was also performed to test the selectivity. The speed of injection during the hybridization process was 0.26 $\mu L.s^{-1}$, each injection lasted for 70 min, the speed of injection during the interaction between the probes and the sample was 0.83 $\mu L.s^{-1}$, and each injection lasted for 20 min.

Results and Discussion

Principle of amplification by linear DNA chain formation

From the existence of two split-aptamers forming sandwich-like structures with the small target adenosine, we developed an original amplification method based on a self-assembling strategy. The latter is based on the formation of linear DNA chains by adenosine bridges between oligonucleotide dimers presenting split-aptamer dangling ends (see **Fig. 1C** and **Fig. 2**). The dimers are formed by the simple hybridization of complementary zipper sequences Z and Zc (see **Fig. 1A**). Those dimers presented at their extremities two dangling ends corresponding to the split-aptamer sequences SX and SX* respectively. Those dimers self-assembled in presence of the adenosine target due to the adenosine bridges formed by the complex between the two split-aptamers and the target. In order to analyze in details the formation of those bridges as function of the target concentration, we studied various split-aptamer sequences S5, S6 and S8 containing respectively 5, 6 and 8 hybridizing bases with their counter-parts S5*, S6* and S8*. Furthermore, to analyze in details the amplification effect, we considered various grafting densities of the probes on the biosensor surface to evaluate the crowding effects on the linear chain formation and to optimize the number of adenosine bridges. Thus, various injection steps were considered for both the detection of adenosine and the determination of the number of adenosine bridges per probe present on the microarray.

In **Step 1**, the stabilization of the microarray with zipper probes Z (red in **Fig 2** Scheme) was obtained by a running buffer injection. This initial microarray allowed us to further implement the different engineered sequences of split-aptamers to obtain functional microarrays and to optimize the number of adenosine bridges. In **Step 2**, the injection of monomer strands SX*Zc

(complementary zipper Zc (red) and split-aptamer SX* (blue) sequences) allowed for their hybridization and led to split-aptamer dangling ends on the microarrays at various grafting densities (see **Fig. 1B**). In **Step 3**, the functional microarray with split-aptamer probes was stabilized upon injection of the running buffer. **Step 4** corresponded to the detection step with the injection of dimers presenting two split-aptamer dangling ends to form linear chains on the microarray due to bridges triggered by the presence of adenosine (see **Fig. 1C** and **Fig. 2**). In **Step 5**, the injection of the running buffer destabilized the adenosine bridges and could regenerate the functional microarray for a subsequent dimer injection and adenosine detection (see paragraph Regeneration of microarrays). A complete regeneration of the microarray (**Step 1**) is also possible upon injection of NaOH solution to dissociate any hybridized strands on the microarray.

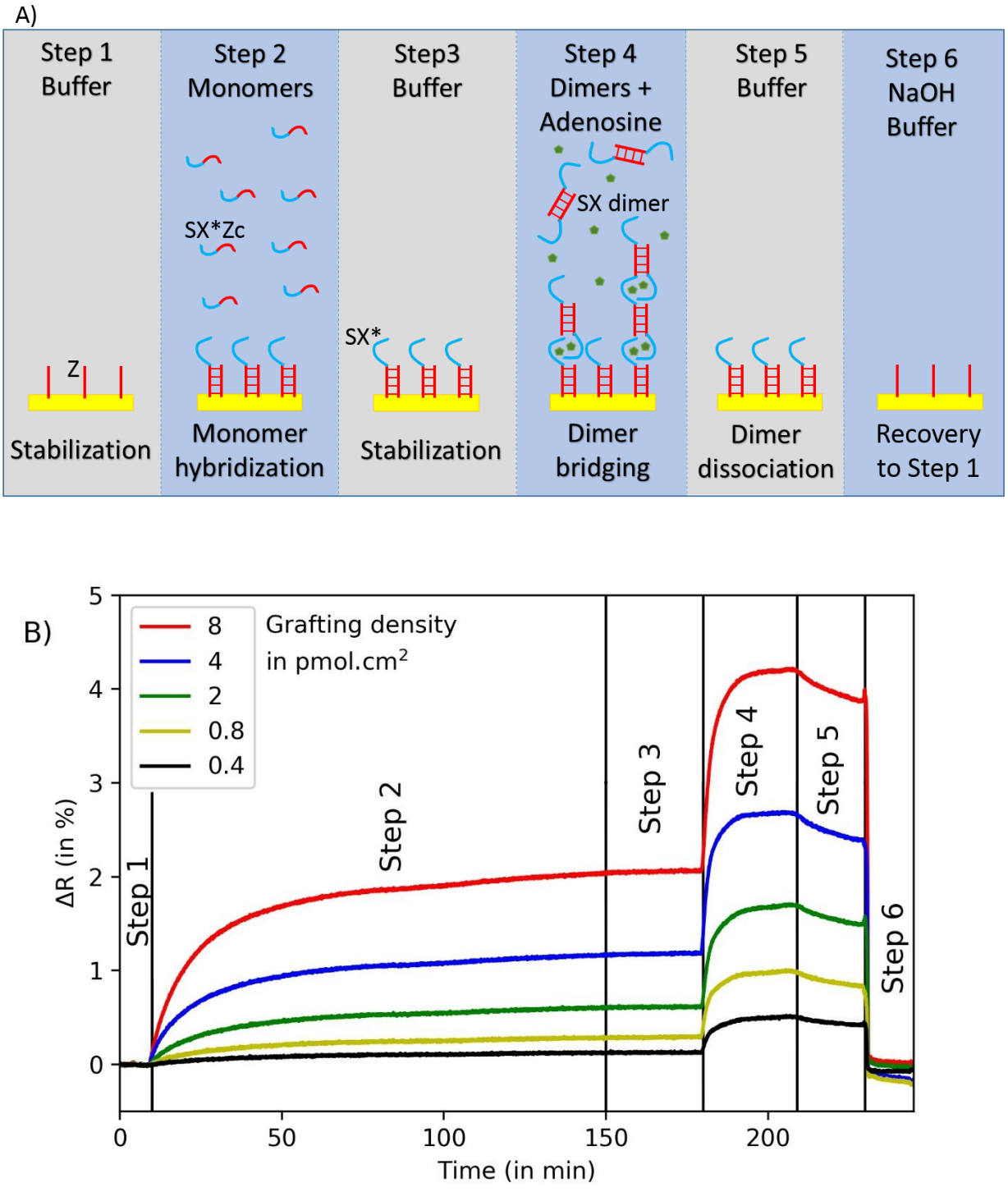

Figure 2 Various injection steps considered for the detection of adenosine and the determination of the number of dimer bridges. **A)** Schematic representation of the various steps and **B)** Corresponding SPR signal. **Step 1**: Stabilization of the initial microarray with zipper probes (red)

by a running buffer injection. **Step 2**: Injection of monomer strands with complementary zipper (red) and split-aptamer (blue) sequences for hybridization and fabrication of functional microarray. **Step 3**: Stabilization of the functional microarray with split-aptamer probes under buffer injection. **Step 4**: Injection of dimers with two split-aptamer dangling ends to form linear chains on the microarrays due to adenosine bridges. **Step 5**: Injection of running buffer removed the adenosine bridges and could regenerate the functional microarray for a subsequent dimer injection and adenosine detection. Step 6: Injection of NaOH buffer removed the hybridized DNA strands to recover the initial microarray (Step 1).

Varying grafting density of probes

Multiple spots with various grafting densities of zipper strands Z were considered on the same microarray. By mixing zipper strands Z and negative control sequences NC, we managed to reach grafting densities in the range 0.4 to 8 pmol.cm^{-2}. The highest density was obtained while applying only zipper strands in the grafting solution. The grafting density was previously confirmed by quantitative radioactive measurement (30) following Herne and Tarlov method (31). Electrochemical determination would have also been possible through the use of $Ru(NH_3)_6^{3+}$ redox label (32). Since a linear dilution of the grafting solution did not lead to a similar linear behavior of the grafting density (30), we varied the grafting density by spotting mixtures of zipper strands Z with negative control sequences NC at a constant total concentration (20 μM of strands). Thus, the grafting densities 8, 4, 2, 0.8, 0.4 pmol.cm^{-2} respectively were obtained by 1, 2, 4, 10 and 20 dilution of Z strands in the grafting solution while complementing by NC strands to keep the total oligonucleotide concentration constant. The stabilization of the microarray was further obtained by an injection of the running buffer (**Step 1**).

From initial to functional microarrays

From such initial microarray with Z probes, it was possible to address any DNA sequence as probes by its simple coupling with Zc, the complementary strand of Z, and further hybridization on the microarray. Thus, an injection of monomer strands SX*Zc were performed to obtain a functional microarray with split-aptamer dangling ends SX* as probes (**Step 2**). The interest of this **Step 2** was twofold for a detailed analysis of the amplification method. First of all, from the initial microarray, we were able to obtain functional microarrays with various split-aptamer sequences depending on the monomer strands injected SX*Zc. Thus, with strong efficiency, the sequence engineering of the split-aptamers was tested on the same microarrays by either injecting S5*Zc, S6*Zc or S8*Zc. An overall regeneration of the microarray is possible by injecting NaOH solution to remove the monomer strands SX*Zc and to recover the initial microarray (**Step 6**). Secondly, **Step 2** also served as a calibration step since the SPR signal observed was useful to further determine the number of bridges and the length of the DNA chains formed in the detection step (**Step 4**). In order for this calibration to be effective, the hybridization of the monomers SX*Zc should be complete (100% hybridization) on every spots and for each grafting density. In the recent literature, the saturation effects due to crowding of the probes have been tested and experimentally observed (33, 34, 35) as well as theoretically analyzed (36, 37, 38). In our study, it seemed that the use of PEG molecules on the probe surfaces favored the probe hybridization even at large grafting densities. This was confirmed by the linear SPR signal ΔR observed as function of the grafting density (**Fig. 3**). The lack of saturation at high grafting densities suggested that 100% of the probes had been hybridized independently of the grafting density. The linear fit of the SPR signal ΔR presented a vanishing value when grafting density went to 0 pmol.cm^{-2}. In other words, when no probe was grafted on the surface, the signal of hybridization was correctly predicted to $\Delta R = 0\%$.

This further confirmed that the hybridization of the probes were complete on all the range of grafting densities studied. Thus, the same grafting density of the functional probes SX* were present at the surface of the microarray than the initial grafting density of the probes Z. Furthermore, the maximum grafting density tested in this study (8 pmol.cm^{-2}) was sufficiently low to avoid crowding effects of the probes and the saturation of the hybridization reaction.

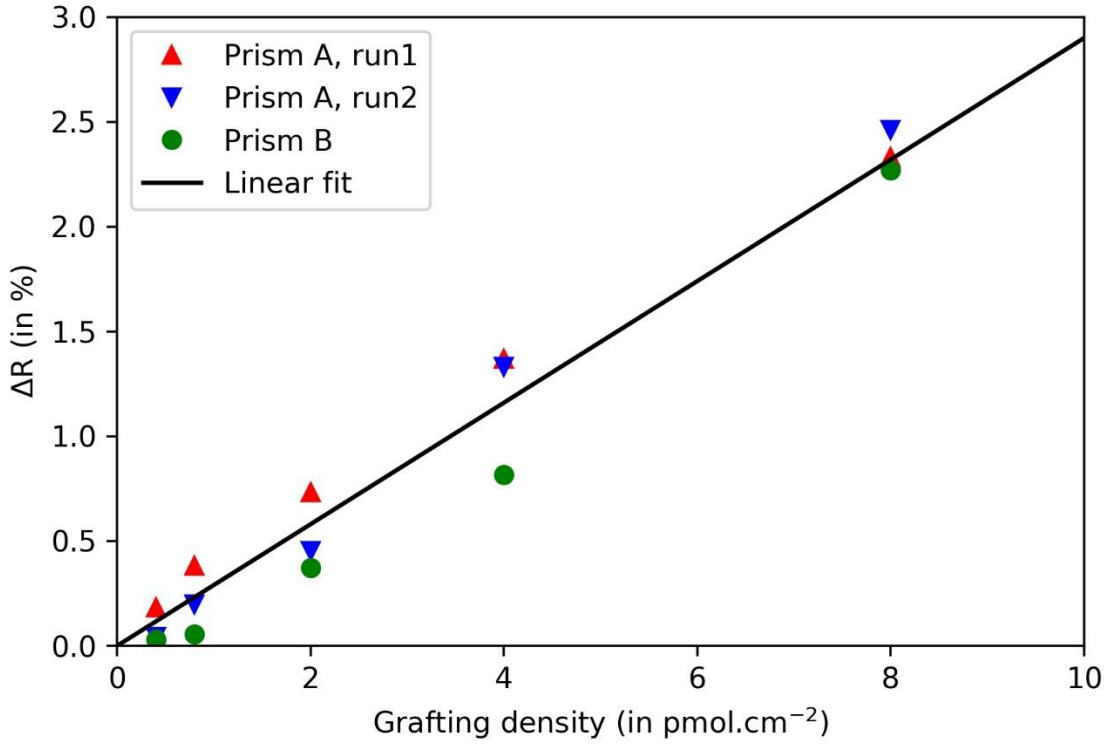

Figure 3 SPR signal obtained following hybridization of monomer injection (S6*Zc) at 1 µM concentration as function of the grafting density. Two injections on the same prism A separated by NaOH regeneration (red and blue triangles) and on a different prism B (green circles) confirmed the reproducibility.

The signal obtained after the first injection (**Step 2**) of different tests on the same prism and on different prisms was compared to test the intra- and inter-microarray reproducibility (**Fig 3**). The results showed good repeatability between different tests.

Detection of adenosine

The detection of adenosine target was based on the SPR signal obtained from the second injection (**Step 4**). The detection signal obtained from different sequence designs and approaches were analyzed (see **Fig. 4**). The S5 and S6 dimers referred to as the duplex formed by the couple of sequences "S5Z+S5*Zc" and "S6Z+S6*Zc" respectively. The signal observed for S6 dimer in presence of 1 mM of adenosine was stronger than that for S5 dimer (red circles compared to red triangles in **Fig. 4**). The main reason for this increased signal may be inferred from the presence of one more binding base pair in the split-aptamer stem inducing stronger interactions with adenosine. However, by increasing the number of hybridizing bases, interactions may also occur even without adenosine due to simple hybridization of the split-aptamer dangling ends. This was explicitly observed for the S6 and S8 dimer injections without adenosine target (see SI Fig. S3).

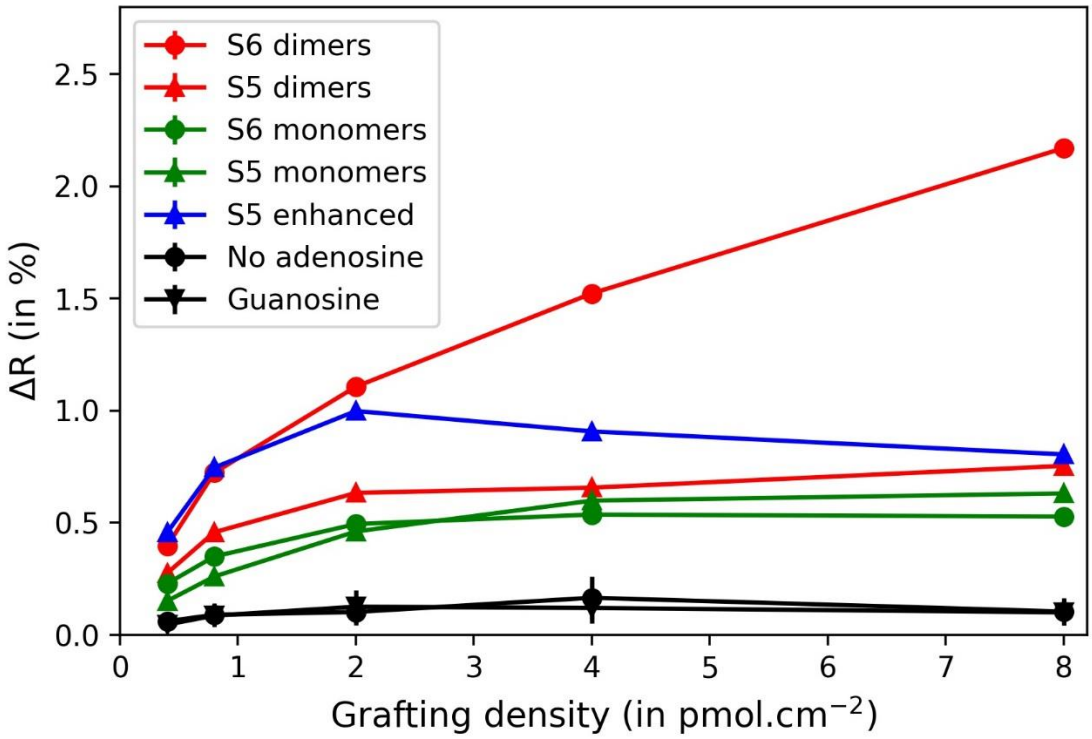

Figure 4 Detection of adenosine by formation of linear chains. SPR signal observed after injection of 1 mM of adenosine and 1 μM of dimers (red) on microarrays with S5-S5* and S6-S6* split-aptamer dangling ends presenting respectively 5 or 6 hybridizing bases (S5 dimer in red triangles or S6 dimer in red circles). As a control, we also represent the SPR signal following injection of 1 mM of adenosine and 1 μM of monomers (green) with split-aptamer dangling ends with respectively 5 or 6 hybridizing bases (S5Z monomers in green triangles or S6Z monomers in green circles). Results for the enhancement strategy with S5Z monomers injection are depicted with blue triangles. Negative controls (in black) correspond to the injection of dimers without targets (circles) or 1 mM concentration of guanine (down triangles) to test the selectivity. Error bars have been determined from the standard deviation of the response of the triplicate spots on the microarray.

The influence of grafting densities on the SPR results has already been discussed in the previous section. With an increase of the grafting density, more probes were available inside the spots. A linear increase of SPR signal after the first injection (**Step 2**) was observed (see **Fig. 3**). The increase of the SPR signal with the grafting density could be observed as well during the second injection (**Step 4**) (**Fig. 4**). However, we observed a non-linear behavior with a saturation for larger grafting densities. This was consistent with a crowding effect during chain formation leading to shorter chains at larger grafting densities. Another explanation may also be the impact of electrostatic interactions. Theoretical models have analyzed that the electrostatic interactions play an important role in the hybridization of DNA on solid support at low salt concentration and high grafting density (36, 37, 38) which has been further demonstrated experimentally (39, 40). Thus, the increased number of probes was counter-balanced by the reduced length of the linear chains formed on the biosensor. This result was also confirmed by the average number of adenosine bridges per probes present on the microarray as function of the grafting density (see section *Number of adenosine bridges*).

There were two negative controls used in this study to confirm the detection of adenosine and the selectivity, respectively. In both cases, the test started with hybridization of S5*Zc monomer sequence on the probes Z to obtain a functional microarray. Then, for the confirmation of adenosine detection, S5 dimers were injected without adenosine (black circles in **Fig 4**). The SPR signal observed after the injection, around 0.1%, was comparable to the biosensor noise and was significantly lower than the signal observed upon injection of adenosine at 1 mM with S5 dimers. This effectively confirmed the detection of adenosine (see the next section for the detection limit). To control the selectivity of the biosensor, S5 dimers were also injected with 1 mM of guanosine. Guanosine is a molecule with similar structure as adenosine but without binding affinity toward

split-aptamer of adenosine. Effectively, the SPR signal observed (black down triangles in **Fig 4**) was similar to the negative control without any target in the buffer, confirming the selectivity of the biosensor toward adenosine.

In order to assess the interest of the linear chain formation in the signal amplification, we also compared the SPR signal upon injection of monomers instead of dimers to avoid the formation of linear chains. We observed similar SPR signals for both S5Z and S6Z monomer injections (sequences S5Z green triangles and S6Z green circles respectively in **Fig 4**) with 1 mM of adenosine. Those signals were increased compare to the two negative controls (lack of adenosine or guanosine injection) especially for grafting densities above 2 $pmol.cm^{-2}$ where the SPR signal reached 0.5% more than 3 times the noise signal. The injection of S6 dimers (red circles) produced even larger SPR signals than S6Z monomers confirming the interest of the self-assembling of linear chains to amplify the sandwich assay in the detection of the small molecule adenosine. However, this enhancement was not recovered for S5 dimer injections which suggested that sequence engineering was necessary to optimize the formation of linear chains.

Since S5 dimer injection did not improve the SPR signal as compared to S5Z monomer injection, we developed an enhancement strategy ("S5 enhanced" **Fig 4**). It was done by the following injection steps: First, similarly as for the classic approach, the S5*Zc sequence was injected to hybridize on the probes immobilized on the gold surface to form S5* functional probes. Then, instead of injecting the duplex formed by S5Z and S5*Zc couple, the duplex formed with S5Z and S6cZc was injected as well as adenosine molecules. This dimer still formed binding with the split aptamer dangling ends S5* on the surface but was limited to only one adenosine bridge formed on each probe and led to a S6c sequence as dangling ends. Then, another injection of the complementary S6c dimer from mixtures of S6Z and S6cZc sequences was made to enhance the

SPR signal. In order to remove the initial adenosine bridge, the presence of 1 mM of adenosine was conserved upon this second injection. The complementary S6c dimer formed linear head-tail self-binding chains where the split aptamer dangling ends are replaced by self-complementary oligonucleotide dangling ends (S6-S6c) to further increase the binding affinity of the bridges. To sum up, this strategy enhanced the SPR signal of S5 dimer by changing the classical adenosine bridges self-assembling mechanism by two kinds of binding mechanisms: 1) Adenosine bridges for the first bound dimer and 2) standard DNA hybridization for the following extension of the linear chains. In **Fig 4**, the SPR signal obtained from "enhanced S5" was 50% higher than the S5 dimer injections at low grafting density of probes (below 2 pmol.cm^{-2}), even close to the S6 dimer injections. However at larger grafting densities (8 pmol.cm^{-2}), the enhancement was not efficient. The spots with 8 pmol.cm^{-2} grafting density had the same SPR signal for S5 dimer injections and enhanced S5 strategy. Therefore, the optimal strategy remains the injection of S6 dimers at every grafting density to perform longer chains.

Regeneration of the microarrays

The regeneration of the microarrays is essential for multiple consecutive detections of adenosine. As can be seen form Fig. 2B, the dissociation of the adenosine bridges formed in Step 4 is relatively low in Step 5 and do not allow for a full regeneration of the functional microarray back to Step 3. Thus, consecutive detections of adenosine would require the regeneration to the initial microarray back to Step 1 by the injection of NaOH solution (Step 6) and the further injection of SX*Zc monomers to recover a functional microarray.

In the case of adenosine detection by injection of S5 dimers, however, the recovery of the functional microarray directly to Step 3 after a buffer injection was possible (see SI Fig. S4). It

allowed us a second adenosine detection (Step 4 B in Fig. S4) at the same concentration of 100 μM than the first one (Step 4 A in Fig. S4). After a second regeneration of the functional microarray, a third adenosine detection was performed at 1 mM (Step 4 C in Fig. S4). The main reason for the fast regeneration to a functional microarray is the lower stability of the adenosine bridges of S5 dimers compared to the S6 and S8 dimers due to the sequence engineering and the lower number of hybridizing bases (5 compared to 6 and 8 respectively).

Number of adenosine bridges

During **Step 2**, the monomers SX*Zc were hybridized on the initial probes Z leaving a split-aptamer dangling end SX* as functional probes for the detection of adenosine. The second injection involved oligonucleotide dimers with SX-SX* split-aptamer dangling ends (**Step 4**). Its injection combined with the presence of adenosine induced the formation of linear DNA chains attached to the functional probes via adenosine bridges. Since the signal increased in SPR measurement was proportional to the mass increase on the surface, the signal from **Step 2** and **Step 4** injections could be used to determine the average length of the linear chains or the average number of adenosine bridges. The SPR signal increase from **Step 2**, ΔR(mono), was proportional to the total mass of the monomers attached onto the surface and thus to the mass of the monomers and the number of initial probes since the hybridization is complete (100% hybridization). The signal increase from **Step 4**, ΔR(dimers), was proportional to the total mass of the dimers that formed the linear chains and thus to the mass of the dimer (twice the mass of the monomer), the number of functional probes (similar to the number of initial probes) and the number of adenosine bridges. Finally, the average number of adenosine bridges, N(bridges), on each probe may simply

be determined by the ratio between ΔR(dimers) and ΔR(mono) as N(bridges) = ΔR(dimers) /2 ΔR(mono). The factor 2 reflects the fact that the dimer mass is twice the monomer one.

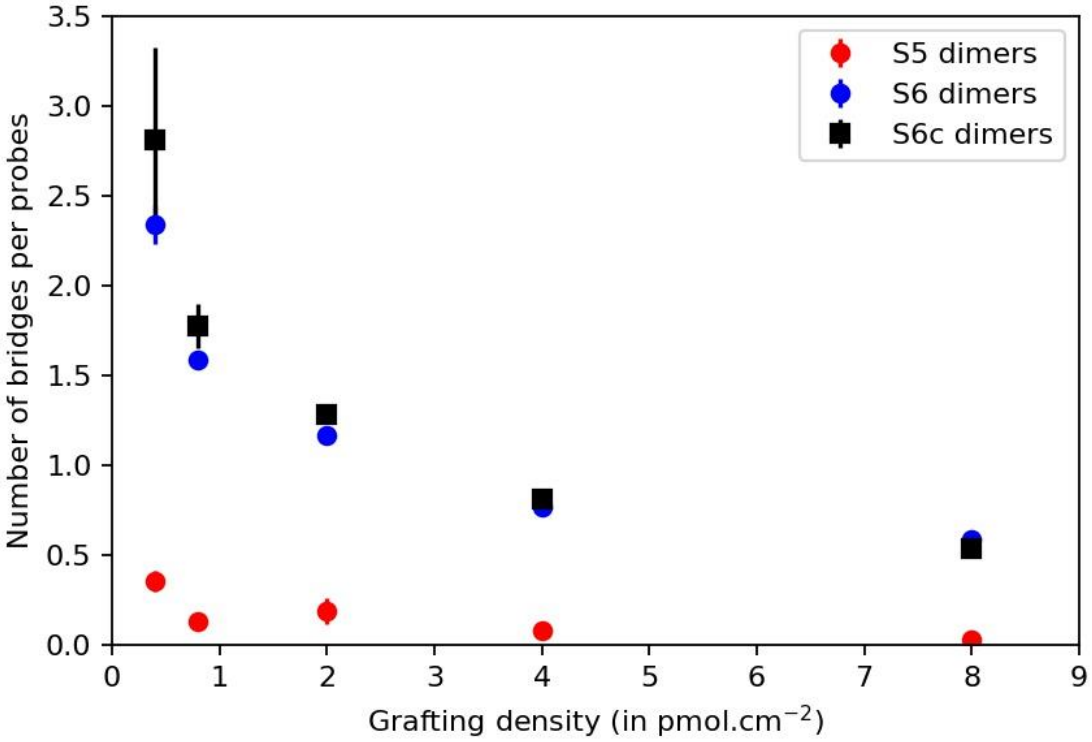

Figure 5 Average number of adenosine bridges as function of the grafting density for an injection of S5 and S6 dimers (red and blue circles) with 100 μM of adenosine and for an injection of S6c dimers (black squares) with S6 and S6c complementary dangling ends. Error bars have been determined from the standard deviation of the response of the triplicate spots on the microarray.

The impact of grafting density on linear chain formation was further studied through the average number of adenosine bridges (see **Fig 5**). A change in the grafting density not only modified the total amount of probes available, but also the average distance between the probes. The fact that the number of bridges was decreasing with the grafting density drew the conclusion that given more space between probes the linear chain had better conditions for growing in length. However,

the loss in the number of probes led to a decrease in the overall SPR signal, regardless of the longer 1D chains on each probe. In fact, from the number of bridges per probe and the grafting density, it is possible to determine the quantity of dimers bounds to the surface. On one hand, at low grafting density (0.4 pmol.cm^{-2}) where the number of bridges per probe is highest (~2.5 for the S6 dimers), 1 pmol.cm^{-2} of dimers are bound to the surface. On the other hand, at high grafting density (8 pmol.cm^{-2}) where the number of bridges per probe is reduced (~0.5 for the S6 dimers), 4 pmol.cm^{-2} of dimers are bound at the surface (4 times more than at low grafting density).

In order to assess that the length of the linear chains was not limited by the concentration of adenosine, we used the injection of the fully complementary S6c dimers as positive control. Since the formation of the bridges is due only to hybridization of self-complementary strands S6-S6c and Z-Zc for the S6c dimers, we expected to obtain the maximum number of bridges. Electrophoresis analysis have shown that while linear chains formed for S6c dimers in solution, they were not stable enough to be observed for S6 dimers even in presence of 1 mM adenosine (see Supplementary Data Fig. S4). However, we observed that S6 and S6c dimers led to similar results suggesting that the number of bridges observed upon injection of S6 dimers is not limited by the concentration of adenosine and the strength of the adenosine bridge for the formation of linear chains at the surface of the biosensor. On the contrary, the results observed for the S5 dimers have shown that the strength of the adenosine bridges were not enough to reach the maximum number of bridges.

Detection limit and selectivity

Surprisingly, even though they were not strong enough for maximal growing length, the S5 dimers led to the best detection limit. In order to assess the detection limit of adenosine molecules by the

current self-assembling strategy of 1D linear chain formations on biosensors, we considered S5 dimer injections at various adenosine concentrations (**Fig 6**). From the SPR signal obtained in the range 0 – 50 μM and the signal noise observed, the limit of detection (LOD) was determined to be 10 μM. This LOD was determined as the concentration for which the signal to noise ratio is 3. This value is comparable to the dissociation constant of the full aptamer (K_D = 6 μM) (21) and well below the estimated value for the split-aptamer (K_D = 50 μM) (27). The detection range was not limited to the linear range 10-50 μM shown on Fig. 6 but may be extended up to 1 mM as shown in SI Fig. S5. An injection of guanosine at 1 mM presented the same signal as without adenosine which confirmed the selectivity of the method. Higher LODs were observed for the dimers S6 and S8 as the result of the higher background signal (see Supplementary Data Fig. S6). With an increasing number of hybridizing bases in the stems of the split-aptamers, a larger SPR signal was obtained for the injection of SX dimers (X = 6 or 8) even without adenosine. This implied a reduced capability to detect minute increase of signal while adding a small amount of adenosine. Thus, better LOD were obtained for the signal OFF (without background SPR signal) to signal ON in presence of adenosine with the S5 dimers. Similar results were observed for sandwich assays using gold nanoparticles (26). Among the assays using the split-aptamers of adenosine, a recent study using Surface Plasmon Field-Enhanced Fluorescent presented a LOD = 42 μM for adenosine (41). In contrary, those using amplifications based on gold nanoparticles for an amplification strategy present a lower LOD (few tens of pM obtained by Melaine et al. (26, 28)). Then, the better sensibility is principally due to multiple bindings and cooperativity effects. In order, to reduce the LOD while avoiding the complex functionalization and use of gold nanoparticles, we may consider within our approach complex DNA structures with more than two dangling ends to form more complex networks than linear chains.

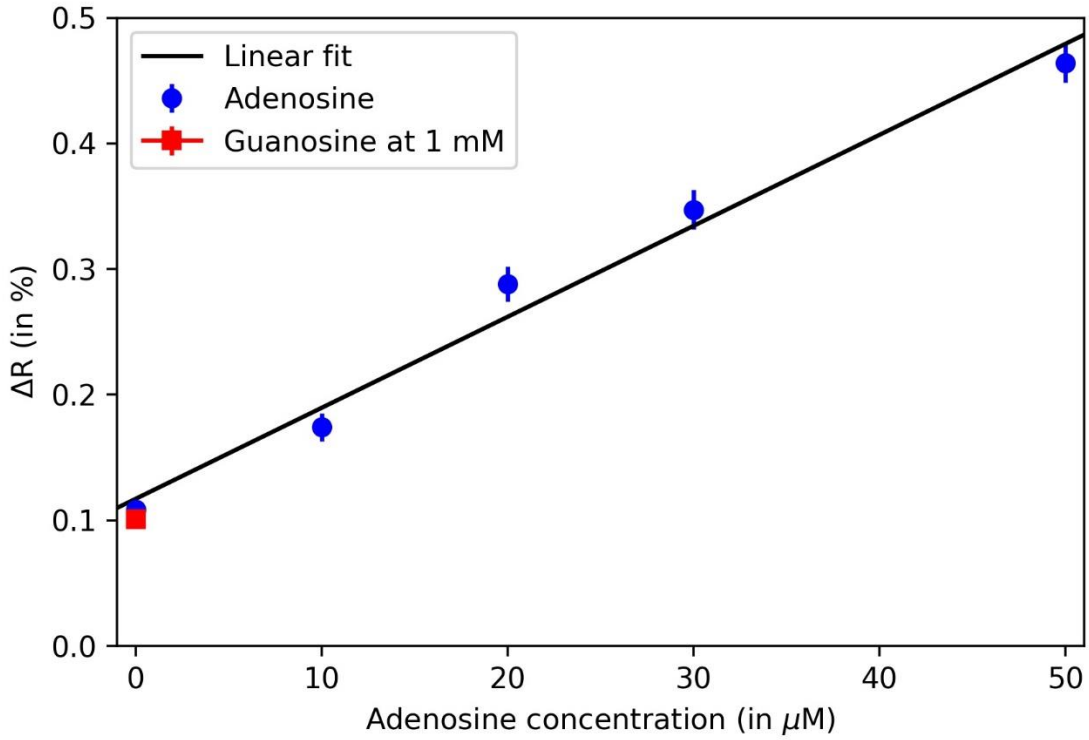

Figure 6 SPR signal for S5 dimer injections as function of adenosine concentration (blue circles) for the spot with grafting density of 8 pmol.cm^{-2}. Guanosine injection at 1 mM served as selectivity control (red square). Error bars have been determined from the standard deviation of the response of the triplicate spots on the microarray.

Conclusion

In order to circumvent the difficulties to detect small molecules with biosensors, we proposed an amplification strategy based on the self-assembly of linear DNA chains triggered by the targets. Although similar strategies might be extended to other molecular targets bound by aptamers, such as proteins, we have chosen to focus on small compounds which are noticeably more challenging to detect on biosensors. In this study, adenosine served as a small molecule model ligand and we considered Surface Plasmon Resonance imaging as the detection technique. Oligonucleotide

dimers presenting split-aptamer dangling ends were injected with the target. After precise sequence engineering of the split-aptamers, it was shown that the presence of adenosine target triggers the formation of bridges between the dimers through split-aptamer dangling ends bonding. The effect of the grating density of the probes on the length of the linear chains formed at the surface of the biosensor was analyzed. It was shown that by decreasing the grafting density, the length of the multi-strand chains increased. However, on the SPR signal, this increase is insufficient to counter-balance the reduction in immobilized probe densities. Thus, higher grafting densities constituted the best option even if they led to shorter multi-strand chains. Furthermore, the sequences leading to the longer chains (S6) were not those leading to the best detection limit of adenosine. This is principally explained by the existence of bridges with S6 sequences even in absence of adenosine that impair the detection of low amount of adenosine. While the detection limit with S5 dimers remains low (LOD = 10 μM), the potential simple regeneration of our approach could be interesting for continuous monitoring of small molecules like recently suggested by Sergelen et al. (41).

In order to enhance the self-assembling amplification, it would be interesting to study the formation of dendritic structures by the use of Y shape or even more complex DNA structures with multiple split-aptamer dangling ends (42, 43). The multiple bindings could help to over-come by cooperative effects the low K_d of the split-aptamers in the formation of large structures linked by adenosine bridges. Finally, it is important to mention that this approach could be generalized to the detection of other small molecules against which split-aptamers could be developed.

ASSOCIATED CONTENT

Supporting Information.

Fig. S1: Glass prisms after grafting solution deposition.

Fig. S2: Image of the microarrays during a Surface Plasmon Resonance imaging experiment.

Fig. S3: Gel electrophoresis analysis of S6 and S6c dimers in solution.

Fig. S4: Regeneration of the functional microarray for successive detections of adenosine.

Fig. S5: Detection range from 10 µM up to 1 mM of adenosine.

Fig. S6: SPR signal of S5, S6 and S8 dimer injections without adenosine targets.

AUTHOR INFORMATION

Corresponding Author

* Arnaud Buhot, Email: arnaud.buhot@cea.fr, Phone +33 4 38 78 38 68.

Author Contributions

The manuscript was written through contributions of all authors. All authors have given approval to the final version of the manuscript. CL performed the experiments and wrote the paper. CSP performed UV absorbance and gel electrophoresis experiments. DG, YR, EP and AB designed the research and all authors participate to the redaction of the paper.

Funding Sources

SyMMES and DPM are part of the Arcane Labex program, funded by the French National Research Agency (ARCANE project no. ANR-12-LABX-003). Chenze Lu was funded by the PhD fellowship program of Arcane Labex.

REFERENCES

1 M. J. Benotti, R. A. Trenholm, B. J. Vanderford, J. C. Holady, B. D. Stanford and S. A. Snyder, Pharmaceuticals and endocrine disrupting compounds in U.S. drinking water. *Environ. Sci. Technol.*, **2009**, *43*, 597–603.

2 R. P. Schwarzenbach, B. I. Escher, K. Fenner, T. B. Hofstetter, C. A. Johnson, U. von Gunten and B. Wehrli, The challenge of micropollutants in aquatic systems. *Science*, **2006**, *313*, 1072–1077.

3 D. R. Spring, Chemical genetics to chemical genomics: small molecules offer big insights. *Chem. Soc. Rev.*, **2005**, *34*, 472–482.

4 I. Willner and M. Zayats, Electronic Aptamer-Based Sensors, *Angew. Chem. Int. Ed.* **2007**, *46*, 6408 – 6418.

5 A. D. Ellington and J. W. Szostak, In vitro selection of RNA molecules that bind specific ligands. *Nature*, **1990**, *346*, 818–822.

6 C. Tuerk and L. Gold, Systematic evolution of ligands by exponential enrichment: RNA ligands to bacteriophage T4 DNA polymerase. *Science*, **1990**, *249*, 505–510.

7 R. M. Dirks and N. A. Pierce, Triggered amplification by hybridization chain reaction. *Proc. Natl. Acad. Sci. USA*, **2004**, *101*, 15275–15278.

8 B. Zhang, B. Liu, D. Tang, R. Niessner, G. Chen, and D. Knopp, DNA-based hybridization chain reaction for amplified bioelectronic signal and ultrasensitive detection of proteins. *Anal. Chem.* **2012**, *84*, 5392−5399.

9 Y. Chen, J. Xu, J. Su, Y. Xiang, R. Yuan, and Y. Chai, In situ hybridization chain reaction amplification for universal and highly sensitive electro-chemiluminescent detection of DNA. *Anal. Chem.* **2012**, *84*, 7750−7755.

10 X. Chen, C.-Y. Hong, Y.-H. Lin, J.-H. Chen, G.-N. Chen, and H.-H. Yang, Enzyme-Free and Label-Free Ultrasensitive Electrochemical Detection of Human Immunodeficiency Virus DNA in Biological Samples Based on Long-Range Self-Assembled DNA Nanostructures. *Anal. Chem.* **2012**, *84*, 8277−8283.

11 P. Liu, X. Yang, S. Sun, Q. Wang, K. Wang, J. Huang, J. Liu, and L. He, Enzyme-Free Colorimetric Detection of DNA by Using Gold Nanoparticles and Hybridization Chain Reaction Amplification, *Anal. Chem.* **2013**, *85*, 7689−7695.

12 F. Wang, B. Willner and I. Willner, DNA nanotechnology with one-dimensional self-assembled nanostructures, *Current Opinion in Biotechnology* **2013**, *24*, 562–574.

13 Z. Ge, M. Lin, P. Wang, H. Pei, J. Yan, J. Shi, Q. Huang, D. He, C. Fan, and X. Zuo, Hybridization Chain Reaction Amplification of MicroRNA Detection with a Tetrahedral DNA Nanostructure-Based Electrochemical Biosensor. *Anal. Chem.* **2014**, *86*, 2124−21.

14 J. S. Kahn, A. Trifonov, A. Cecconello, W. Guo, C. Fan, and I. Willner, Integration of Switchable DNA-Based Hydrogels with Surfaces by the Hybridization Chain Reaction, *Nano Lett.* **2015**, *15*, 7773−7778.

15 A. Trifonov, E. Sharon, R. Tel-Vered, J. S. Kahn, and I. Willner, Application of the Hybridization Chain Reaction on Electrodes for the Amplified and Parallel Electrochemical Analysis of DNA, *J. Phys. Chem. C* **2016**, *120*, 15743−15752.

16 L. Zou, R. Li, M. Zhang, Y. Luo, N. Zhou, J. Wang and L. Ling, A colorimetric sensing platform based upon recognizing hybridization chain reaction products with oligonucleotide modified gold nanoparticles through triplex formation. *Nanoscale*, **2017**, *9*, 1986–1992.

17 Q. Guo, F. Bian, Y. Liu, X. Qu, X. Hu and Q. Sun, Hybridization chain reactions on silica coated Qbeads for the colorimetric detection of multiplex microRNAs. *Chem. Commun.,* **2017**, *53*, 4954-4957.

18 A. Sato, K. Terata, H. Miura, et al. Mechanism of vasodilation to adenosine in coronary arterioles from patients with heart disease. *Am J Physiol Heart Circ Physiol*., **2005**, 288, H1633-H1640.

19 F. Costa, and I. Biaggioni, Role of nitric oxide in adenosine-induced vasodilation in humans. *Hypertension.* **1998**, 62, 1035-1042.

20 J. M. Morgan, D. G. McCormack, M. J. Griffiths, et al., Adenosine as a vasodilator in primary pulmonary hypertension. *Circulation*. **1991**, 84, 1145-1149.

21 D. E. Huizenga and J. W. Szostak, A DNA aptamer that binds adenosine and ATP. *Biochemistry*, **1995**, *34*, 656–665.

22 C. H. Lin and D. J. Patel, Structural basis of DNA folding and recognition in an AMP-DNA aptamer complex: distinct architectures but common recognition motifs for DNA and RNA aptamers complexed to AMP. *Chem. Biol.*, **1997**, *4*, 817–832.

23 F. Li, J. Zhang, X. Cao, L. Wang, D. Li, S. Song, B. Ye and C. Fan, Adenosine detection by using gold nanoparticles and designed aptamer sequences. *Analyst*, **2009**, *134*, 1355–1360.

24 X. Zuo, Y. Xiao and K. W. Plaxco, High Specificity, Electrochemical Sandwich Assays Based on Single Aptamer Sequences and Suitable for the Direct Detection of Small-Molecule Targets in Blood and Other Complex Matrices, *J. Am. Chem. Soc.*, **2009**, 131 (20), 6944–6945.

25 L. Kashefi-Kheyrabadi and M. A. Mehrgardi, Aptamer-conjugated silver nanoparticles for electrochemical detection of adenosine triphosphate, *Biosensors Bioelectron.* **2012**, 37, 94–98.

26 F. Melaine, Y. Roupioz and A. Buhot, Gold Nanoparticles Surface Plasmon Resonance Enhanced Signal for the Detection of Small Molecules on Split-Aptamer Microarrays. *Microarrays*, **2015**, *4*, 41–52.

27 C. Yang, N. Spinelli, S. Perrier, E. Defrancq, E. Peyrin, Macrocyclic host-dye reporter for sensitive sandwich-type fluorescent aptamer sensor. *Anal. Chem.* **2015**, *87*, 3139-43.

28 F. Melaine, C. Coilhac, Y. Roupioz and A. Buhot, A nanoparticle-based thermo-dynamic aptasensor for small molecule detection. *Nanoscale*, **2016**, *8*, 16947-16954.

29 C. Daniel, F. Mélaïne, Y. Roupioz, T. Livache and A. Buhot, Real time monitoring of thrombin interactions with its aptamers: insights into the sandwich complex formation. *Biosens. Bioelectron.*, **2013**, *40*, 186–192.

30 C. Daniel, Y. Roupioz, D. Gasparutto, T. Livache and A. Buhot, Solution-Phase vs Surface-Phase Aptamer-Protein Affinity from a Label-Free Kinetic Biosensor. *PLoS One*, **2013**, *8*, e75419.

31 T. M. Herne, and M. J. Tarlov, Characterization of DNA Probes Immobilized on Gold Surfaces, *J. Am. Chem. Soc.* **1997**, 119, 8916-8920.

32 A. B. Steel, T. M. Herne, and M. J. Tarlov, Electrochemical Quantitation of DNA Immobilized on Gold, *Anal. Chem.* **1998**, 70, 4670-4677.

33 T. J. Petty, C. E. Wagner and A. Opdahl, Influence of Attachment Strategy on the Thermal Stability of Hybridized DNA on Gold Surfaces. *Langmuir* **2014**, *30*, 15277−15284.

34 H.-C. Chiang and R. Levicky, Effects of Chain–Chain Associations on Hybridization in DNA Brushes. *Langmuir* **2016**, *32*, 12603−12610.

35 L. J. A. Macedo, E. N. Miller and A. Opdahl, Effect of Probe−Probe Distance on the Stability of DNA Hybrids on Surfaces. *Anal. Chem.* **2017**, *89*, 1757−1763.

36 A. Halperin, A. Buhot and E. B. Zhulina, Sensitivity, specificity, and the hybridization isotherms of DNA chips. *Biophys. J.* **2004**, *86*, 718–730.

37 A. Halperin, A. Buhot and E. B. Zhulina, On the hybridization isotherms of DNA microarrays: the Langmuir model and its extensions. *J. Phys.: Condensed Matter* **2006,** *18*, S463-S490.

38 A. Harrison et al., Physico-Chemical Foundations Underpinning Microarray and Next-Generation Sequencing Experiments. *Nucleic Acids Res* **2013**, *41*, 2779-2796.

39 P. Gong, R. Levicky, DNA surface hybridization regimes. *Proc Natl Acad Sci U S A.* **2008**, 105, 5301-6.

40 J. Fuchs, J. B. Fiche, A. Buhot, R. Calemczuk, T. Livache, Salt concentration effects on equilibrium melting curves from DNA microarrays. *Biophys J.* **2010**, 99, 1886-95.

41 K. Sergelen, B. Liedberg, W. Knoll and J. Dostálek, Surface plasmon field-enhanced fluorescence reversible split aptamer biosensor, *Analyst*, **2017**, 142, 2995-3001.

42 H.-M. Meng, H. Liu, H. Kuai, R. Peng, L. Moa and X.-B. Zhang, Aptamer-integrated DNA nanostructures for biosensing, bioimaging and cancer therapy. *Chem. Soc. Rev.* **2016**, *45*, 2583-2602.

43 X. Ding, W. Cheng, Y. Li, J. Wu, X. Li, Q. Cheng, S. Ding, An enzyme-free surface plasmon resonance biosensing strategy for detection of DNA and small molecule based on nonlinear hybridization chain reaction. *Biosens. Bioelectron.* **2017**, *87*, 345-351.

BRIEFS (Word Style “BH_Briefs”). If you are submitting your paper to a journal that requires a brief, provide a one-sentence synopsis for inclusion in the Table of Contents.

SYNOPSIS (Word Style “SN_Synopsis_TOC”). If you are submitting your paper to a journal that requires a synopsis, see the journal’s Instructions for Authors for details.

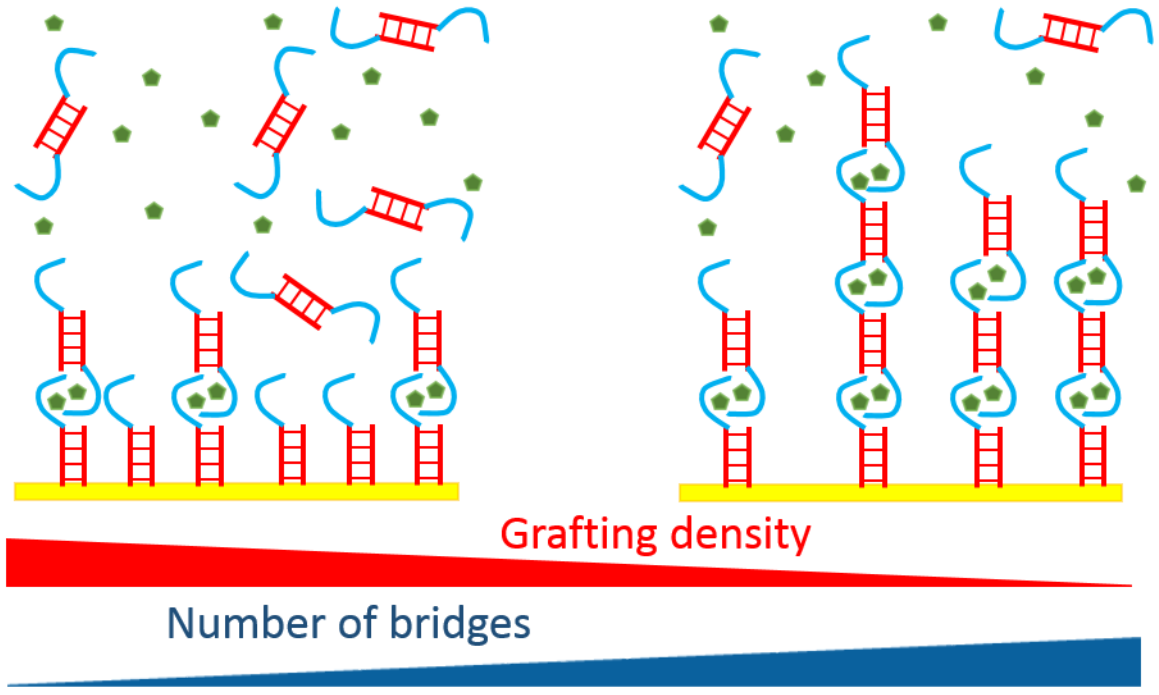

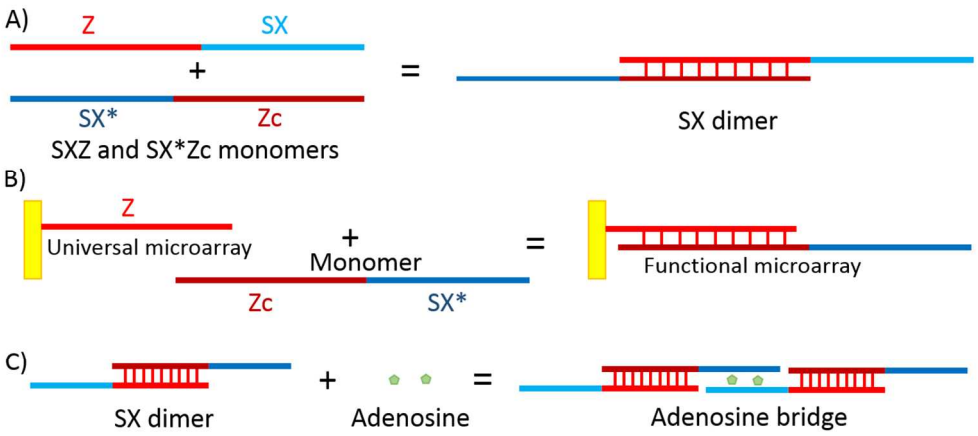

Scheme of the strands and their interactions. A) Monomer strands formed of Z+SX and Zc+SX* with X = 5, 6 or 8 complementary bases between SX and SX*. SX* may also be replaced by SXc the fully complementary strand of SX. Due to the fully complementary strands Z and Zc, the two monomers form dimers in solution. B) From an initial microarray with Z strand probes at various grafting densities, a functional microarray may be obtained by the injection of monomers SX*Zc leading to SX* dangling end probes. C) The addition of adenosine target in presence of dimers on functional microarrays allows for the formation of linear chains by adenosine bridges.

229x108mm (150 x 150 DPI)

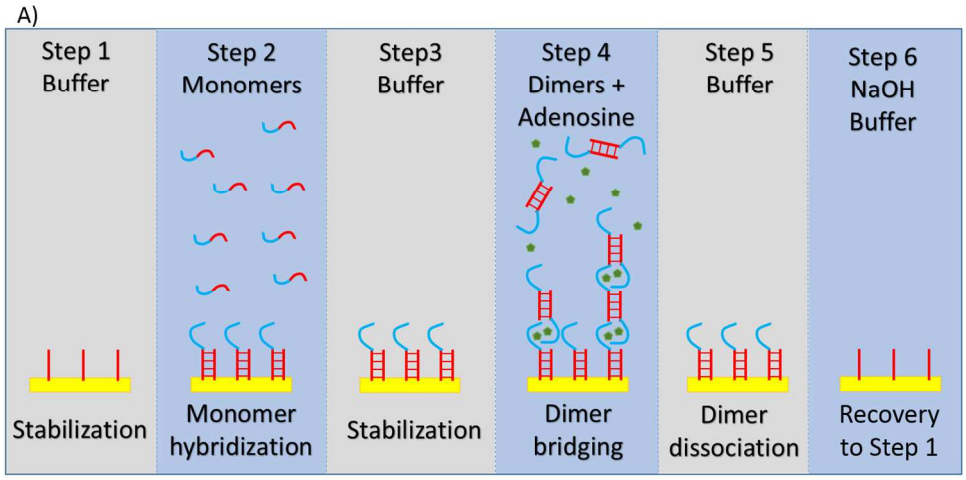

Various injection steps considered for the detection of adenosine and the determination of the number of dimer bridges. A) Schematic representation of the various steps and B) Corresponding SPR signal. Step 1: Stabilization of the initial microarray with zipper probes (red) by a running buffer injection. Step 2: Injection of monomer strands with complementary zipper (red) and split-aptamer (blue) sequences for hybridization and fabrication of functional microarray. Step 3: Stabilization of the functional microarray with split-aptamer probes under buffer injection. Step 4: Injection of dimers with two split-aptamer dangling ends to form linear chains on the microarrays due to adenosine bridges. Step 5: Injection of running buffer removed the adenosine bridges and could regenerate the functional microarray for a subsequent dimer injection and adenosine detection. Step 6: Injection of NaOH buffer removed the hybridized DNA strands to recover the initial microarray (Step 1).

259x129mm (150 x 150 DPI)

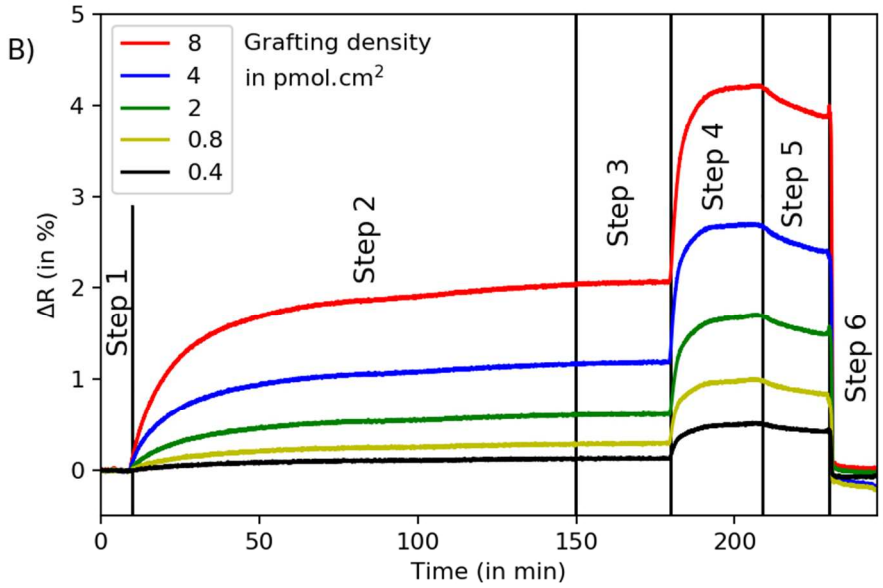

Various injection steps considered for the detection of adenosine and the determination of the number of dimer bridges. A) Schematic representation of the various steps and B) Corresponding SPR signal. Step 1: Stabilization of the initial microarray with zipper probes (red) by a running buffer injection. Step 2: Injection of monomer strands with complementary zipper (red) and split-aptamer (blue) sequences for hybridization and fabrication of functional microarray. Step 3: Stabilization of the functional microarray with split-aptamer probes under buffer injection. Step 4: Injection of dimers with two split-aptamer dangling ends to form linear chains on the microarrays due to adenosine bridges. Step 5: Injection of running buffer removed the adenosine bridges and could regenerate the functional microarray for a subsequent dimer injection and adenosine detection. Step 6: Injection of NaOH buffer removed the hybridized DNA strands to recover the initial microarray (Step 1).

152x101mm (160 x 160 DPI)

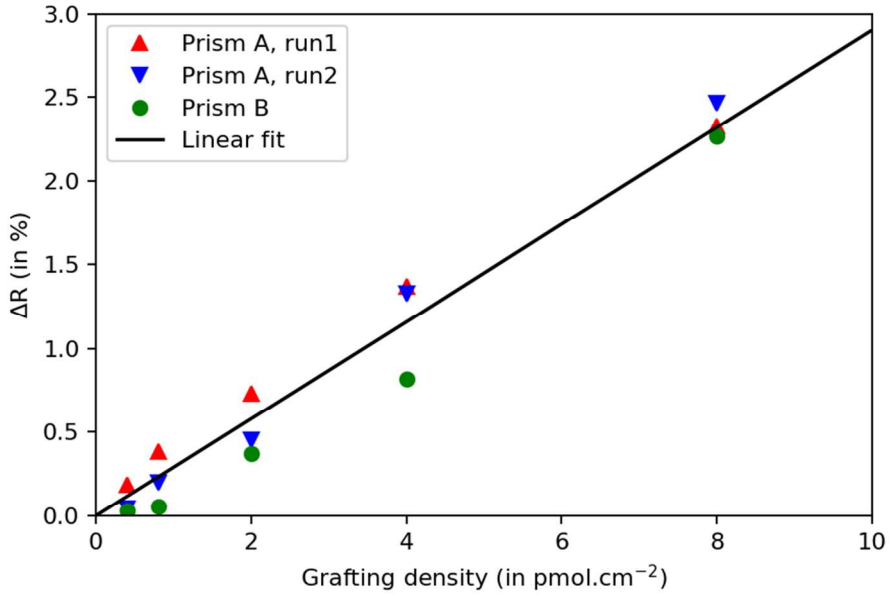

SPR signal obtained following hybridization of monomer injection (S6*Zc) at 1 µM concentration as function of the grafting density. Two injections on the same prism A separated by NaOH regeneration (red and blue triangles) and on a different prism B (green circles) confirmed the reproducibility.

152x101mm (160 x 160 DPI)

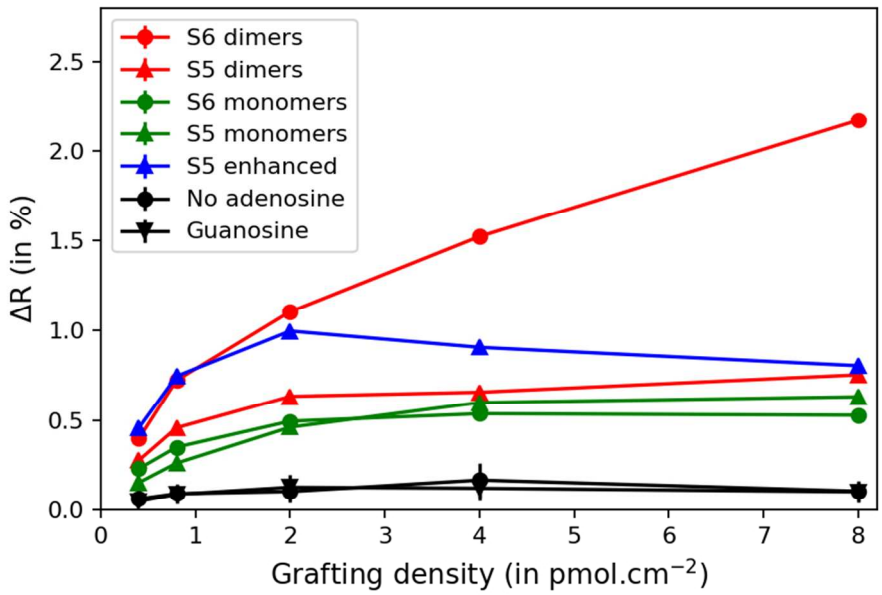

Detection of adenosine by formation of linear chains. SPR signal observed after injection of 1 mM of adenosine and 1 µM of dimers (red) on microarrays with S5-S5* and S6-S6* split-aptamer dangling ends presenting respectively 5 or 6 hybridizing bases (S5 dimer in red triangles or S6 dimer in red circles). As a control, we also represent the SPR signal following injection of 1 mM of adenosine and 1 µM of monomers (green) with split-aptamer dangling ends with respectively 5 or 6 hybridizing bases (S5Z monomers in green triangles or S6Z monomers in green circles). Results for the enhancement strategy with S5Z monomers injection are depicted with blue triangles. Negative controls (in black) correspond to the injection of dimers without targets (circles) or 1 mM concentration of guanine (down triangles) to test the selectivity. Error bars have been determined from the standard deviation of the response of the triplicate spots on the microarray.

152x101mm (160 x 160 DPI)

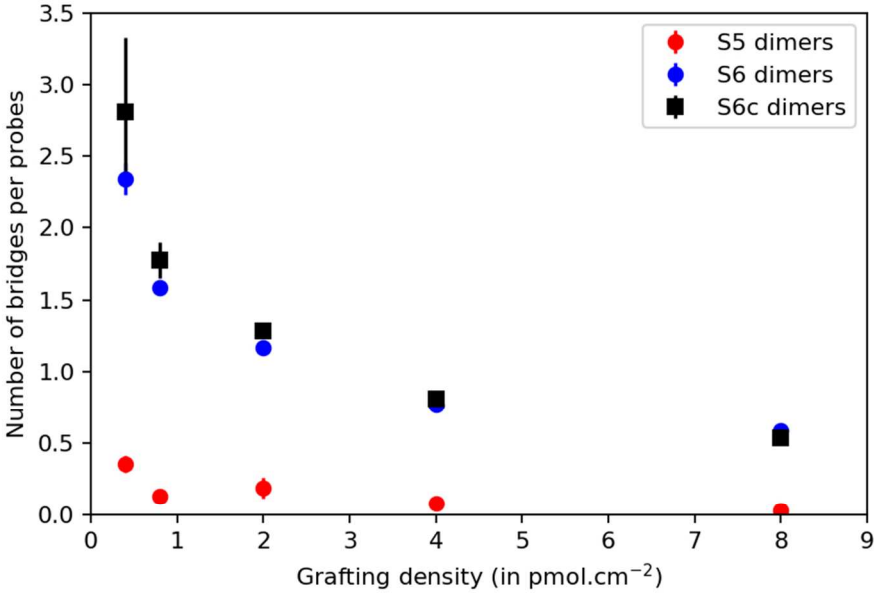

Average number of adenosine bridges as function of the grafting density for an injection of S5 and S6 dimers (red and blue circles) with 100 M of adenosine and for an injection of S6c dimers (black squares) with S6 and S6c complementary dangling ends. Error bars have been determined from the standard deviation of the response of the triplicate spots on the microarray.

152x101mm (160 x 160 DPI)

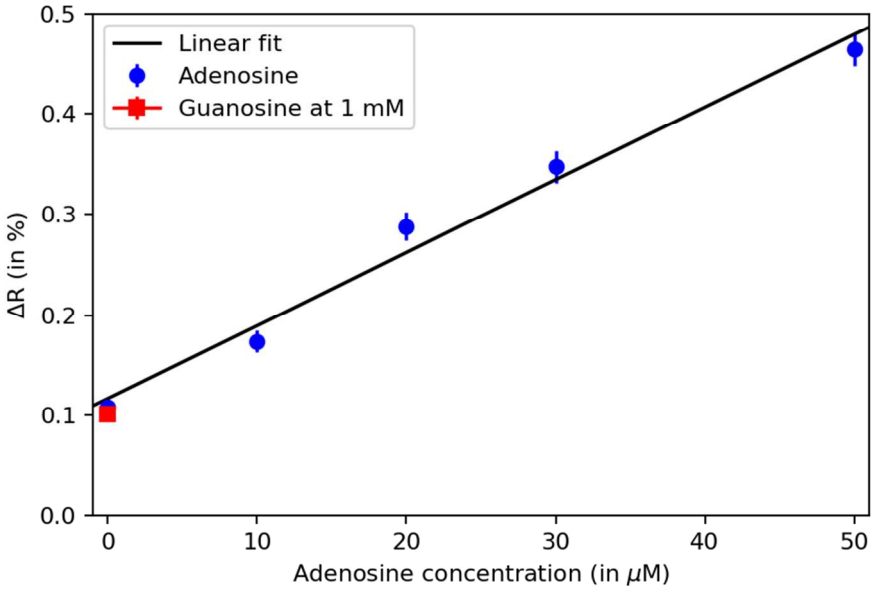

SPR signal for S5 dimer injections as function of adenosine concentration (blue circles) for the spot with grafting density of 8 pmol.cm-2. Guanosine injection at 1 mM served as selectivity control (red square). Error bars have been determined from the standard deviation of the response of the triplicate spots on the microarray.

152x101mm (160 x 160 DPI)

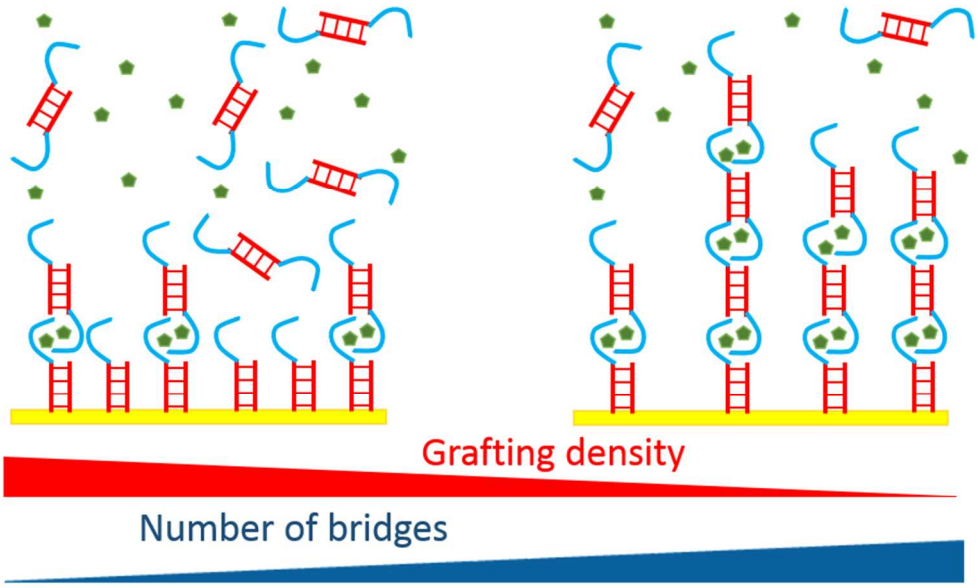

TOC Graphics

156x96mm (150 x 150 DPI)